

X-ray Bursts from the Accreting Millisecond Pulsar XTE J1814-338

Tod E. Strohmayer¹, Craig B. Markwardt², Jean H. Swank¹, and Jean in 't Zand³

ABSTRACT

Since the discovery of the accreting millisecond pulsar XTE J1814-338 a total of 27 thermonuclear bursts have been observed from the source with the Proportional Counter Array (PCA) onboard the Rossi X-ray Timing Explorer (RXTE). Spectroscopy of the bursts, as well as the presence of continuous burst oscillations, suggests that all but one of the bursts are sub-Eddington. The remaining burst has the largest peak bolometric flux of 2.64×10^{-8} erg s⁻¹cm⁻², as well as a gap in the burst oscillations, similar to that seen in Eddington limited bursts from other sources. Assuming this burst was Eddington limited we obtain a source distance of ≈ 8 kpc. All the bursts show coherent oscillations at the 314.4 Hz spin frequency. The burst oscillations are strongly frequency and phase locked to the persistent pulsations. Only two bursts show evidence for frequency drift in the first few seconds following burst onset. In both cases the initial drift corresponds to a spin down of a few tenths of a Hz. The large oscillation amplitude during the bursts confirms that the burst flux is modulated at the spin frequency. We detect, for the first time, a significant first harmonic component in burst oscillations. The ratio of countrate in the first harmonic to that in the fundamental can be > 0.25 and is, on average, less than that of the persistent pulsations. If the pulsations result from a single bright region on the surface, the harmonic strength suggests the burst emission is beamed, perhaps due to a stronger magnetic field than in non-pulsing LMXBs. Alternatively, the harmonic content could result from a geometry with two bright regions.

Subject headings: binaries: general – stars: individual (XTE J1814-338) – stars: neutron – stars: rotation – X-rays: bursts - X-rays: stars

¹Laboratory for High Energy Astrophysics, NASA's Goddard Space Flight Center, Greenbelt, MD 20771
email: stroh, swank@milkyway.gsfc.nasa.gov

²LHEA/University of Maryland, College Park, MD 20772 email: craigm@milkyway.gsfc.nasa.gov

³SRON National Institute for Space Research, Sorbonnelaan 2, NL - 3584 CA Utrecht, the Netherlands,
email: jeanz@sron.nl

1. Introduction

Recently, Markwardt & Swank (2003) reported the discovery of the fifth accreting millisecond pulsar, XTE J1814-338 (hereafter J1814). This pulsar has a 314.36 Hz spin frequency, resides in a binary with an orbital period of 4.275 hours, and has a minimum companion mass of $\approx 0.15M_{\odot}$ (Markwardt et al. 2003). This is the widest, and most massive binary of the 5 known accreting millisecond pulsars. The system parameters of J1814 closely match those of the “classical”, non-pulsing low mass X-ray binaries (LMXBs), for example the 3.8 hour binary 4U 1636-53. These systems are not generally observed as persistent pulsars, but the neutron star spins are known from the detection of oscillations during thermonuclear bursts (see Strohmayer & Bildsten 2003 for a review of burst oscillations). Evidence is emerging that the accreting millisecond pulsars must have stronger large scale magnetic fields than the non-pulsing LMXBs (Galloway et al. 2002; Cumming, Zweibel & Bildsten 2001). The fundamental quantity controlling the field strength may be the long term accretion rate, if the accretion can “bury” the field. These pulsars are all transients and/or subluminescent compared to other LMXBs, suggesting a lower long term accretion rate. Magnetic fields also play a key role in the frequency stability of burst oscillations (Cumming, Zweibel & Bildsten 2001). Detailed studies of J1814 and its bursts may thus provide insight into the magnetic fields of LMXBs, and why some do not show persistent pulsations.

The recent discoveries of coherent oscillations during a superburst from 4U 1636-53 (Strohmayer & Markwardt 2002), and burst oscillations from the millisecond pulsar SAX J1808.4-3658 (hereafter J1808, Chakrabarty et al. 2003), have conclusively established that the frequency of burst oscillations are directly related to the spin of the neutron star. Since the discovery of J1814 in June, 2003 extensive observing with RXTE has been undertaken. At the time of this writing a total of 27 thermonuclear bursts have been observed. Pulse trains at the 314.36 Hz spin frequency have been detected in all of these bursts, making this source the second for which burst oscillations have been observed at the known spin frequency of the neutron star. In this Letter we report on a study of these first bursts observed from J1814. As we show below, the burst oscillations are phase locked to the persistent pulsations. We find good evidence for frequency drifting near the onset of only two of the bursts. Most interestingly, we detect the first significant harmonic structure in burst oscillation waveforms. We use spectroscopy of the bursts to obtain a distance constraint. We conclude with some discussion of the implications of our findings.

2. Burst Time Profiles and Spectroscopy

Some basic properties of a representative sample of the bursts are given in Table 1. Almost all the bursts last typically 2 minutes and are characterized by a rise time (as defined by the time it takes the photon count rate to grow from 10% to 100% of the peak value) of 5 to 10 seconds, and $1/e$ decay times, as measured from the peak onward, of 20 to 35 seconds. Two different temporal components are present: a bright and fast component with peak rates above $600 \text{ c s}^{-1}\text{PCU}^{-1}$ and durations of at most 30 seconds, and a slow component that is responsible for the overall duration. The weak bursts appear to lack the fast component. The timescale of the longer component suggests that the neutron star is accreting hydrogen-rich material at a rate where stable hydrogen burning is either not occurring (implying $\dot{m} < 9 \times 10^2 \text{ g cm}^{-2}\text{s}^{-1}$) or the burning rate is too slow to catch up with the supply of fresh fuel (implying $\dot{m} > 2 \times 10^3 \text{ g cm}^{-2}\text{s}^{-1}$; Fujimoto, Hanawa & Miyaji 1981, Fushiki & Lamb 1987; Cumming & Bildsten 2000). The peak count rate, corrected for pre-burst persistent levels and evaluated with 0.5 second time resolution, ranges between ≈ 0.4 to $1.4 \text{ kcts s}^{-1}\text{PCU}^{-1}$. Burst 27, the last burst observed, is qualitatively different from the others in that its rise time is shorter, and it reached a higher peak flux. These differences suggest a higher fraction of helium fuel for this burst. If stable hydrogen burning were taking place prior to this burst, then the lower \dot{m} at this epoch should have allowed for more of the accumulating hydrogen to burn, perhaps resulting in a higher helium fraction.

The background-subtracted spectral data could be well fitted with single temperature black body radiation and a negligible absorbing column, n_{H} . The evolution of the temperature and black body radius are similar for most bursts, except that the peak temperatures of the fainter bursts, and burst 27, are ≈ 1.7 and 3 keV , while all others are in the range from 2.3 to 2.5 keV . None of the bursts convincingly show spectroscopic evidence of photospheric radius expansion. Therefore all bursts, with the exception of burst 27, appear to be sub-Eddington. This is also consistent with the presence of burst oscillations throughout the peaks of these bursts (Muno et al. 2002). Again, burst 27 is different in that its burst oscillations show a gap across the peak (see Figure 1, top right). Such gaps are seen in many radius expansion bursts with oscillations (Muno et al. 2002), suggesting that burst 27 reached the Eddington limit. As noted above, this burst also had the highest peak color temperature, $> 3 \text{ keV}$, of any of the bursts. If this burst was indeed Eddington limited then we get a distance constraint based on the peak bolometric flux of $2.64 \times 10^{-8} \text{ erg s}^{-1}\text{cm}^{-2}$. Assuming an Eddington limit of $2 \times 10^{38} \text{ erg s}^{-1}$ (for a canonical neutron star and a hydrogen dominated photosphere) we get a distance of $\approx 8 \text{ kpc}$. The uncertainty on this distance is estimated to be roughly 20% (Kuulkers et al. 2003).

2.1. Burst Oscillations

For all the bursts we have 125 μ -sec time resolution PCA event mode data. We first barycentered the data using the JPL DE405 solar system ephemeris and the source position determined from PCA scans (Markwardt & Swank 2003). Our timing analysis is performed using the Z_n^2 statistic (Buccheri et al. 1983; Strohmayer & Markwardt 2002). We first computed dynamic power spectra for each burst. We used 4 s intervals to compute Z_1^2 , and we started a new interval every 0.25 seconds. Significant oscillations were detected in each burst in the vicinity of the 314 Hz pulsar frequency. The pulse trains during most of the bursts lasted from 30 - 100 seconds. These are longer than the pulse trains observed from most burst oscillation sources, and allow the time evolution of the pulsed amplitude to be explored in some detail. Most bursts show complex, episodic modulations in the amplitude of $\approx 3 - 5\%$ (rms) on timescales ranging from 7 - 15 s. We will explore this interesting behavior in more detail in a sequel. The dynamic spectra indicate that the frequency during most bursts is stable, showing little evidence for the drifting seen in other sources (Strohmayer & Markwardt 1999; Munro et al. 2002).

We performed a phase coherent timing analysis for each burst. We used a linear frequency evolution model, $\nu(t) = \nu_0 + \delta\nu t$ (ie. the phase is quadratic in time), to model the phase of the oscillations. We tracked the phases in successive time bins throughout each burst and found the values of ν_0 and $\delta\nu$ which gave the best fit to the data. The best fit is found by minimizing $\chi^2 = \sum_{i=1}^N (\phi_i(\nu_0, \delta\nu) - \mu)^2 / \sigma_{\phi_i}^2$, where $\mu = (1/N) \sum_{i=1}^N \phi_i(\nu_0, \delta\nu)$, ϕ_i is the phase deduced for the i th bin using the model parameters and all X-ray events in the bin, and N is the number of phase bins.

For each burst the linear frequency model gave an acceptable fit to the phase timing data, and in no case was there a need for a linear drift term, $\delta\nu$, larger than the local change in frequency due to orbital motion. Figure 1 shows dynamic power spectra (top) and phase timing residuals (bottom) for bursts 11 and 27. These were the two bursts which showed significant episodes of frequency drift. In both bursts the frequency evolution shows a spin-down of a few tenths of Hz near the onset of the burst, followed by a statistically weaker recovery (spin up). This behavior appears contrary to that found for J1808, which showed a rapid, few Hz spin up during the rise of a burst (Chakrabarty et al. 2003), although the observed spin up in J1808 might conceivably be related to the recovery phase of the evolution seen in J1814. Nevertheless, the magnitude of the frequency change was much larger in J1808 (≈ 4 Hz). The observation of spin downs in J1814 seems atypical of bursters in general, since most observed drifts are spin ups (see Munro et al. 2002).

We compared the best fitting values for ν_0 for bursts 1 - 12 with the predicted frequency of the persistent pulsations based on the orbital solution of Markwardt et al. (2003). The

results for these 12 bursts are shown in Figure 2. The frequencies of the oscillations during each burst are consistent with the predicted, orbitally modulated, pulsar frequency. Not only are the frequencies consistent, but the phase of the burst oscillations is strongly locked to that of the persistent pulsations. In Figure 3 we compare the phase folded pulse profile from the first 56 ksecs of non-burst data (thick solid curve) with the co-added pulse profiles from bursts 2 and 3. The burst data were folded with the same ephemeris as the persistent pulse data. Both the fundamental and 1st harmonic components of the profile are aligned. Typical 1σ upper limits to any average phase offsets during bursts for the fundamental and 1st harmonic components are ≈ 0.7 and 1.2% , respectively. These limits are smaller than the corresponding phase offset for bursts from J1808 of $\approx 11\%$ (Chakrabarty et al. 2003).

We computed the average amplitudes of the burst oscillations from the phase folded pulse profiles (see Table 1). We define the amplitude as $a = (I_{max} - I_{min}) / (I_{max} + I_{min})$, where I is the countrate of the folded profile. For these estimates we have not subtracted off the preburst, persistent emission. Doing so would increase the amplitudes modestly. The amplitudes are in the range from 14 - 18 %, except for burst 27, which showed systematically weaker oscillations. This is larger than the amplitude of the persistent pulsations, which ranges from about 9 - 12 % when measured in the same way after first subtracting off the detector background. This confirms that the black body burst flux *must* be modulated at the spin frequency. If it were not the amplitude during the bursts would be less than 1%.

The burst oscillations also show a significant harmonic component in their pulse profiles. We demonstrate this in Figure 4, which shows the co-added pulse profile from bursts 2 and 3, as well as a model fit using two Fourier components. The solid curve is the best model, while the dashed and dotted lines show the fundamental and first harmonic components. The harmonic component is strongly required, with an amplitude of 36 ± 2.6 counts s^{-1} . Co-adding bursts 2 and 3 in phase gives $Z_1^2 = 95.2$ at the first harmonic. Since Z_1^2 is distributed as χ^2 with two degrees of freedom, the value of 95.2 is a highly significant detection. The harmonic content varies significantly from burst to burst. When expressed as the ratio of pulsed amplitude at the first harmonic to that at the fundamental, it ranges from essentially 0 - 0.27. We note that this is always less than the harmonic content of the persistent pulsations, for which the same ratio is ≈ 0.33 . In terms of countrate the first harmonic component for the persistent pulsations around the epoch of bursts 2 and 3 is about 4.5 counts s^{-1} , which is much too small to account for the harmonic content during these bursts.

3. Discussion and Summary

J1814 is now the second pulsar to show burst oscillations at the spin frequency of the neutron star. The large amplitude of the modulations confirms that the burst flux is spin modulated, as first suggested by Strohmayer et al. (1996). As in J1808 (Chakrabarty et al. 2003), the phase of the burst oscillations in J1814 are linked to the phase of the persistent pulsations. It seems likely that this phasing results from the magnetic field of the neutron star. In persistent pulsars the magnetic field must be strong enough to channel the accretion flow and produce an asymmetric accretion luminosity. Such a field would then likely also influence the surface distribution of nuclear fuel, resulting in a thermonuclear flux distribution during bursts which tracks the magnetic field geometry. A strong field will also enforce co-rotation of the surface layers, minimizing shearing and thus frequency drifting. The fact that the burst oscillation sources which do not show persistent pulsations also have the frequency drifts with the longest relaxation time seems consistent with this idea (Strohmayer & Markwardt 1999).

Chakrabarty et al. (2003) found evidence for frequency drifting at the onset of a burst from J1808. Although most of the bursts from J1814 that we have examined show no strong evidence of drifting, bursts 11 and 27 are the exceptions. These bursts show evidence for phase drifting near burst onset (Figure 2, lower panels). For these bursts both the phase residuals and the dynamic power spectra suggest that the oscillation frequency was initially higher than the spin frequency and then decreased below the spin frequency before recovering again. For both bursts the evolution takes place in an ≈ 5 s interval during the burst rise.

Perhaps the most interesting result is the detection of significant harmonic content in the burst oscillations. Two important conclusions are that the harmonic content must be intrinsic to the modulation of the thermonuclear flux, and secondly, the harmonic content of the burst oscillations, expressed as the ratio of power at the first harmonic to that at the fundamental, is always less than the harmonic content of the persistent pulsations. As noted by several authors (Strohmayer et al. 1998; Miller & Lamb 1998; Weinberg, Miller & Lamb 2001; Munro et al. 2002), the harmonic content of burst oscillations can in principle be used to constrain the neutron star radius. This is because of the relativistic effects caused by the high surface velocities of these pulsars. The bursts from J1814 with the highest first harmonic content have a harmonic to fundamental ratio greater than 0.25. In contrast, upper limits on this ratio in other burst oscillation sources can be as small as 0.05 (Munro et al. 2002). For a 10 km neutron star, $v_{surf} \approx 0.07c$ for the spin frequency of J1814. At this velocity such a large harmonic ratio is extremely difficult to produce if the emission is isotropic from a single bright region on the neutron star surface (Weinberg, Miller & Lamb 2001; Munro, Ozel & Chakrabarty 2002). Our results suggest that substantial beaming of

the radiation likely occurs if the modulation is from a single bright region on the surface. Alternatively, a geometry with two antipodal bright regions is possible. Detailed modeling of the energy dependent pulse profiles could provide constraints on the stellar compactness, radius and perhaps the magnetic field strength and geometry.

REFERENCES

- Buccheri, R. et al. 1983, *A&A*, 128, 245.
- Chakrabarty, D. et al. 2003, *Nature*, 424, 42.
- Cumming, A., Zweibel, E. & Bildsten, L. 2001, 557, 958.
- Cumming, A. & Bildsten, L. 2000, *ApJ*, 544, 453.
- Fujimoto, M. Y., Hanawa, T., & Miyaji, S. 1981, *ApJ*, 247, 267.
- Fushiki, I. & Lamb, D. Q. 1987, *ApJ*, 323, L55.
- Galloway, D. K., Chakrabarty, D., Morgan, E. H. & Remillard, R. A. 2002, *ApJ*, 576, L137.
- in 't Zand, J. J. M. et al. 2001, *A&A*, 372, 916.
- Kuulkers, E., den Hartog, P. R., in 't Zand, J. J. M., Verbunt, F. W. M., Harris, W. E. & Cocchi, M. 2003, *A&A*, 399, 663.
- Lewin, W. H. G., van Paradijs, J. & Taam, R. E. 1993, *Space Sci. Rev.*, 62, 223.
- Markwardt, C. B., Swank, J. H., Strohmayer, T. E., & in 't Zand, J. J. M. 2003, *ApJ*, in preparation.
- Markwardt, C. B. & Swank, J. H. 2003, *IAUC*, 8144.
- Miller, M. C. & Lamb, F. K. 1998, *ApJ*, 499, L37.
- Muno, M. P., Chakrabarty, D., Galloway, D. K., & Psaltis, D. 2002, *ApJ*, 580, 1048.
- Muno, M. P., Ozel, F. & Chakrabarty, D. 2002, *ApJ*, 581, 550.
- Strohmayer, T. E. & Bildsten, L., in *Compact Stellar X-ray Sources* (eds. Lewin, W. H. G. & van der Klis, M.) (Cambridge Univ. Press, in press); (astro-ph/0301544).
- Strohmayer, T. E. & Markwardt, C. B., 1999, *ApJ*, 516, L81.
- Strohmayer, T. E. & Markwardt, C. B., 2002, *ApJ*, 581, 577.
- Strohmayer, T. E., et al. 1996, *ApJ*, 469, L9.
- Strohmayer, T. E., Zhang, W., Swank, J. H., White, N. E. & Lapidus, I. 1998a, *ApJ*, 498, L135.

Weinberg, N., Miller, M. C. & Lamb, D. Q. 2001, ApJ, 546, 1098.

4. Figure Captions

Fig. 1.— Summary of timing behavior for two representative bursts from J1814 (bursts 11 and 27 in Table 1). The top panels show contour plots of dynamic power spectra computed with the Z_1^2 statistic. The time intervals for the spectra were 4 s in length and a new interval was started every 0.25 s. The bottom panels show the phase residuals for the best fitting constant frequency model. Note the phase modulations near the onset of each burst. In addition to the gap in the pulse train for burst 27, it also had the weakest oscillation of any burst and no detected harmonic.

Fig. 2.— Comparison of the measured burst oscillation frequencies (error bar symbols), and the predicted pulsar frequency based on the orbital Doppler modulation (diamonds). The horizontal and dashed solid lines mark the pulsar rest frame frequency, and the upper and lower frequency limits from the binary motion, respectively. The measured frequencies are consistent with the predicted values.

Fig. 3.— Comparison of pulse profiles for the persistent pulsations (solid), and the co-added profiles for bursts 2 and 3 (histogram). The phases of the burst data were computed using the same orbital ephemeris as for the persistent pulsations. The fact that the profiles are aligned to a high degree demonstrates that the burst oscillations are phase locked to the persistent pulsations.

Fig. 4.— Co-added pulse profile for the sum of bursts 2 and 3 (histogram with error bars). Also shown are the best fitting, two Fourier component model (solid), and the individual contributions from the fundamental (dashed) and first harmonic (dotted) components. The harmonic component has a strength of 36 ± 2.6 counts s^{-1} and is strongly required by the data. The model gives an excellent fit, with a minimum $\chi^2 = 19.4$ with 25 degrees of freedom. Two cycles are shown for clarity.

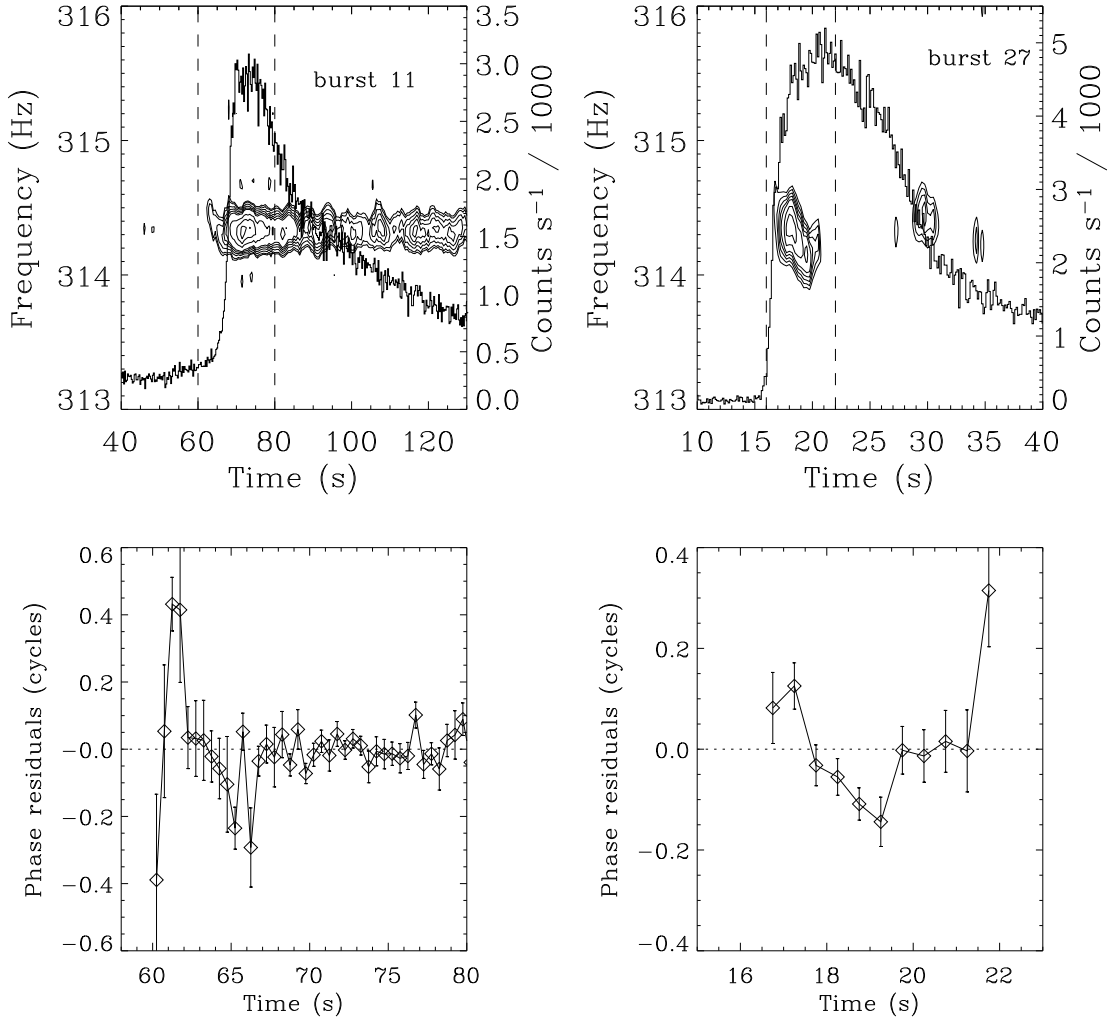


Figure 1: Summary of timing behavior for two representative bursts from J1814 (bursts 11 and 27 in Table 1). The top panels show contour plots of dynamic power spectra computed with the Z_1^2 statistic. The time intervals for the spectra were 4 s in length and a new interval was started every 0.25 s. The bottom panels show the phase residuals for the best fitting constant frequency model. Note the phase modulations near the onset of each burst. In addition to the gap in the pulse train for burst 27, it also had the weakest oscillations of any burst and no detected harmonic.

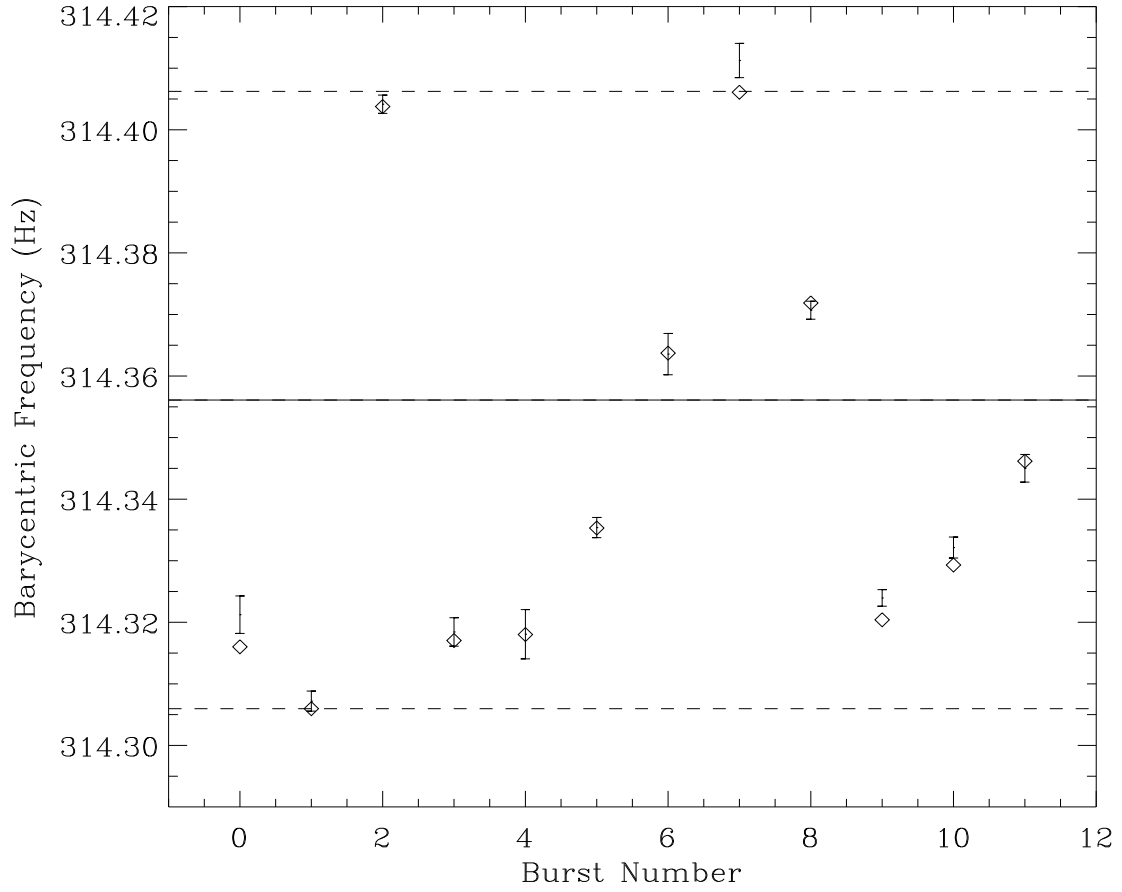


Figure 2: Comparison of the measured burst oscillation frequencies (error bar symbols), and the predicted pulsar frequency based on the orbital Doppler modulation (diamonds). The horizontal and dashed solid lines mark the pulsar rest frame frequency, and the upper and lower frequency limits from the binary motion, respectively. The measured frequencies are consistent with the predicted values.

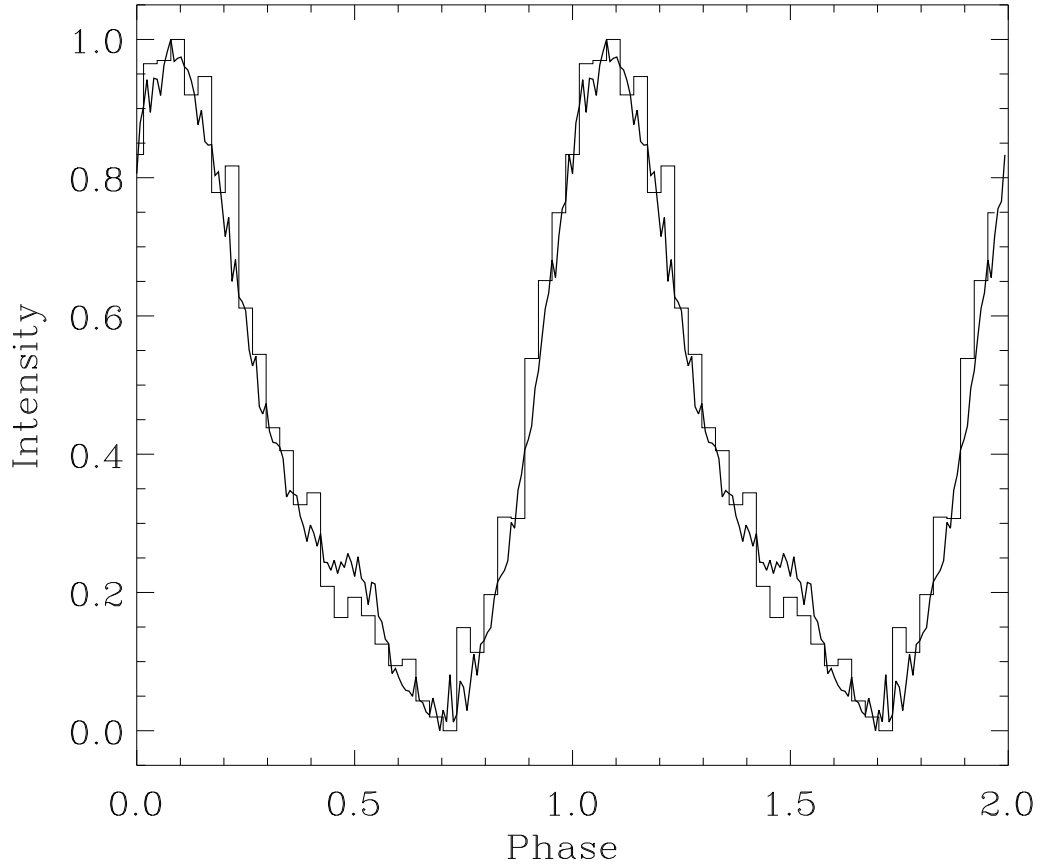


Figure 3: Comparison of pulse profiles for the persistent pulsations (solid), and the co-added profiles for bursts 2 and 3 (histogram). The phases of the burst data were computed using the same orbital ephemeris as for the persistent pulsations. The fact that the profiles are aligned to a high degree demonstrates that the burst oscillations are phase locked to the persistent pulsations.

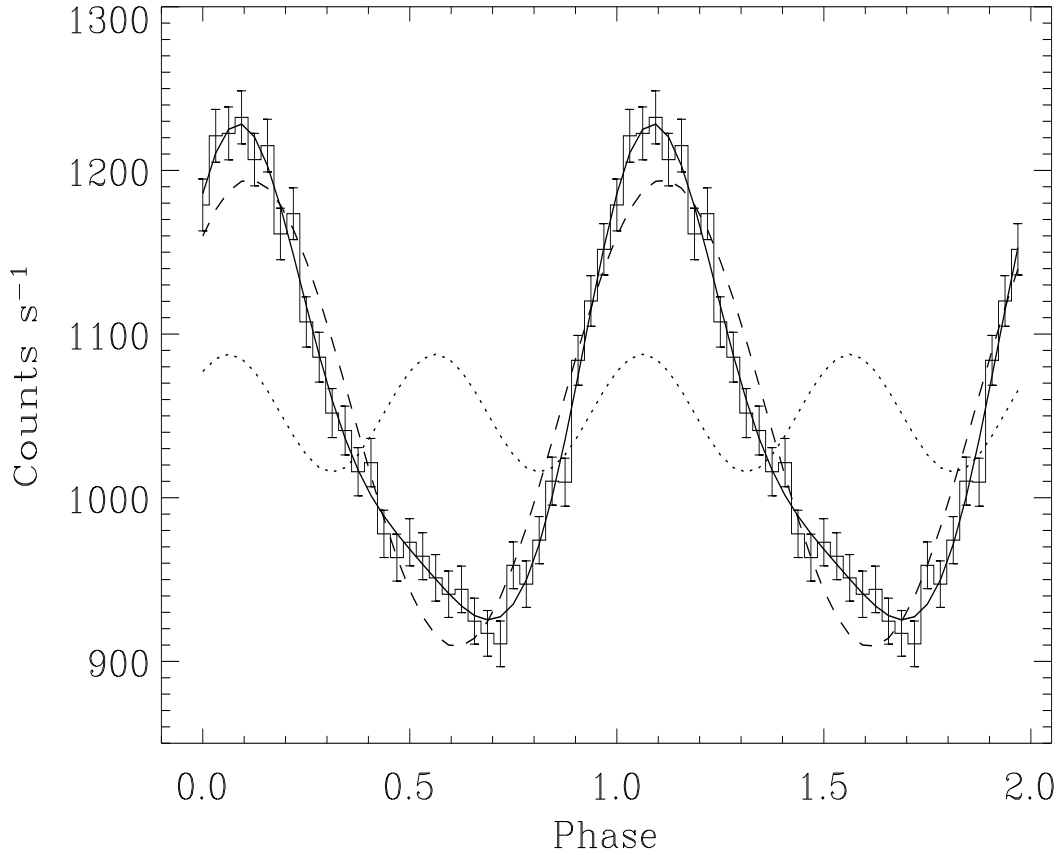


Figure 4: Co-added pulse profile for the sum of bursts 2 and 3 (histogram with error bars). Also shown are the best fitting, two Fourier component model (solid), and the individual contributions from the fundamental (dashed) and first harmonic (dotted) components. The harmonic component has a strength of 36 ± 2.6 counts s^{-1} and is strongly required by the data. The model gives an excellent fit, with a minimum $\chi^2 = 19.4$ with 25 degrees of freedom. Two cycles are shown for clarity.

Table 1: Spectroscopy and Pulse Timing Results for Bursts from J1814

Burst index	Peak time ¹	Peak flux ²	1/e time (sec) ³	Average radius ⁴	Oscillation Frequency ⁵	Average Amplitude ⁶	Harmonic Content ⁷
1	6.0407	0.41±0.05	22.5±0.5	6.75±0.12	314.321	0.139	0.040
2	7.2687	1.25	33.3	6.71	314.307	0.148	0.081
3	7.8836	1.36	32.3	6.81	314.404	0.162	0.053
4	9.1963	1.18	32.4	6.64	314.318	0.181	0.036
5	10.0993	1.44	30.9	6.25	314.318	0.147	0.063
6	11.0293	0.36	25.6	6.07	314.335	0.165	0.047
7	12.4665	0.87	34.3	6.33	314.364	0.176	0.035
8	13.0594	0.40	28.8	6.22	314.411	0.145	0.078
9	13.7342	0.95	33.2	6.36	314.371	0.156	0.026
10	14.0145	1.00	34.8	6.32	314.324	0.146	0.018
11	15.7895	0.84	35.1	6.32	314.332	0.155	0.015
12	16.7475	0.85	38.4	6.20	314.345	0.177	0.044
27	17.7435	2.64	29.4	6.07	314.323	0.10	–

¹Date in June 2003 (UTC), except for burst 27, which is July 2003 (UTC)

²Bolometric, in units of 10^{-8} erg s⁻¹cm⁻², evaluated with 4 s resolution

³ exponential decay time for the slow component of the burst profile

⁴averaged over 40 sec time interval after the peak of each burst, in km for a distance of 10 kpc.

⁵Barycentric frequency in Hz.

⁶Average pulsation amplitude, defined as $(I_{max} - I_{min})/(I_{max} + I_{min})$

⁷Ratio of Z^2 power at the first harmonic to that at the fundamental, if harmonic detected.